Microstructure-Properties relationship in AISI 316L stainless steel produced by wire additive manufacturing (WAAM & WLAM): experimental study and simulation

Thesis defended by Damien ARTIÈRES

on April 11, 2025

Director: Vladimir ESIN
Supervisors: Sylvain DÉPINOY, Serge PASCAL

1. Introduction

General Context

Additive Manufacturing: cost-efficient for producing complex components at low production volumes [Levy et al., 2003].

General context at CEA

Part of an R&D program to evaluate additive manufacturing processes and their application to the nuclear industry.

Additive Manufacturing technologies:

- Powder Bed: most often Laser-Powder Bed Fusion (L-PBF);
- Directed Energy Deposition (DED): shape of material ⇒ powder or wire; energy source ⇒ laser, electrical arc or electron beam.

Process selection

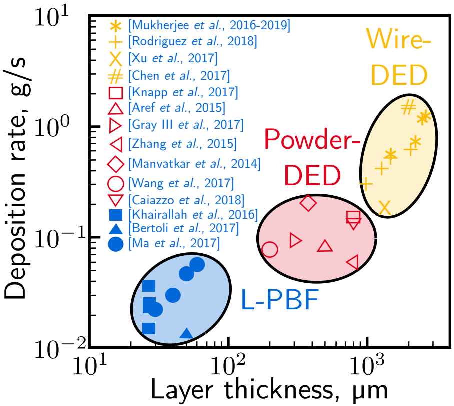

Adapted from [Mukherjee and DebRoy, 2019b].

Wire-DED less studied/industrialized.

Studied processes at CEA/LTA:
WAAM (Wire Arc Additive Manufacturing)
WLAM (Wire Laser Additive Manufacturing)

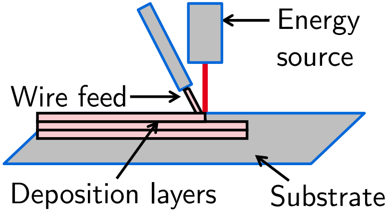

Adapted from [Frazier, 2014].

Potential applications in the nuclear industry

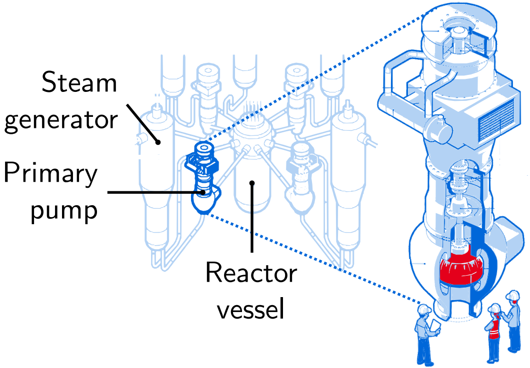

Reactor and associated cooling pump.
Adapted from [IRSN, 2016].

$\rightarrow$ Size $\sim 1 - 10$ m.

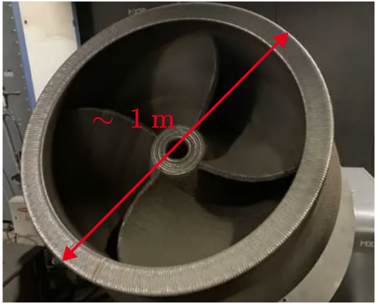

Reactor cooling pump impeller, WAAM.
From [Framatome].

Applications-related constraints

WAAM and WLAM processes

WLAM: metre-sized components, better surface finish compared to WAAM.
⇒ Objectives for the CEA: characterization and comparison of both processes.

Material: AISI 316L austenitic stainless steel → Material of interest to the nuclear industry and model material for additive manufacturing.

Mechanical properties: ensure comparable properties than those of components produced by conventional processes.

Geometry: complex components composed of thin (walls) and thick (tiles) zones.

Manufacturing defects: thermal and mechanical fields monitoring.

Thesis objectives

Objectives

Master the microstructure and geometry of simple 316L steel components manufactured by WAAM and WLAM, and identify construction conditions for the production of full-size components.

1. What are the parameters for manufacturing defect-free components?
2. What are the differences in properties and microstructure between WAAM and WLAM components, and between walls and blocks?
3. Can a finite element model be developed to simulate both processes?

Approach

1. Manufacturing simple components using WAAM and WLAM processes.
   - Determine manufacturing parameters (single beads analysis).
   - Avoid manufacturing defects (geometry, microstructure).
2. Characterizing the manufactured components.
   - Determine and compare the mechanical properties of the components.
   - Establish the microstructure specificities (walls vs tiles; WAAM vs WLAM).
3. Modeling of the processes.
   - Predict relevant fields in manufacturing (temperature, stress, strain).
   - Contribute to the control of the processes.

2. Processing conditions

Objective

What are the parameters for manufacturing defect-free components?

WAAM and WLAM platforms at CEA/LTA

WAAM - Tungsten Inert Gas (TIG) welding.
WLAM - Coaxial laser.

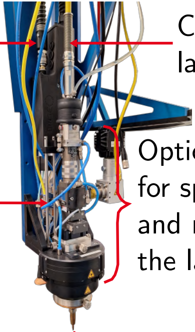

Surface state of 100 mm-high wall

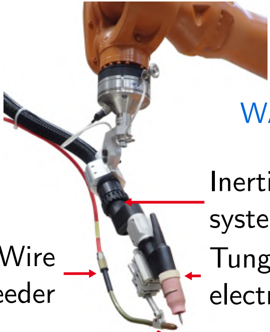

Influence of manufacturing parameters on geometry

Geometry: width, w, height, h, depth into substrate, p.

- Deposition speed, s ;
- wire feed speed, v_w ;
- power of the heat source, Q_{exp}.

Manufacturing parameters influencing the:

- linear energy, $E_l \propto \frac{Q_{exp}}{s}$;
- transverse cross-section, $S \propto \frac{v_w}{s}$;
- volume energy, $E_v \propto \frac{Q_{exp}}{v_w}$;
- deposition rate, $d_{rate} \propto v_w$.

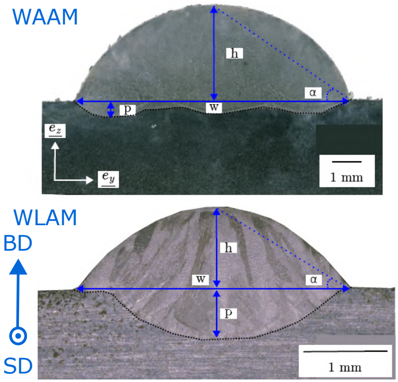

BD: Building Direction; SD: Scanning Direction

Selected process parameters

Measurement of the geometrical dimensions of regular single-beads and selection.

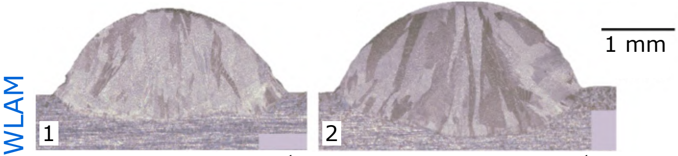

$d_{rate} = 18.1$ g.min^{-1} $\quad$ $d_{rate} = 25.3$ g.min^{-1}

$E_l = 180$ J.mm^{-1} $\quad$ $E_l = 210$ J.mm^{-1}

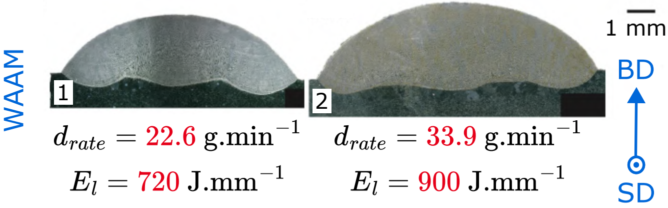

$d_{rate} = 22.6$ g.min^{-1} $\quad$ $d_{rate} = 33.9$ g.min^{-1}

$E_l = 720$ J.mm^{-1} $\quad$ $E_l = 900$ J.mm^{-1}

WLAM	Q_{exp} (W)	s (mm.min^{-1})	v_w (mm.min^{-1})
1	2400	800	2000
2	3500	1000	2800

WAAM	Q_{exp} (W)	s (mm.min^{-1})	v_w (mm.min^{-1})
1	2400	200	2500
2	3000	200	3750

WLAM-1 et WAAM-2 used for component manufacturing.
Deposition rate et repeatability.

Manufacturing of single-bead walls and tiles

Other parameters to calibrate during the manufacturing of components: deposition strategy, interlayer cooling times.

20-layer single-bead walls | **6×20-layer tiles**

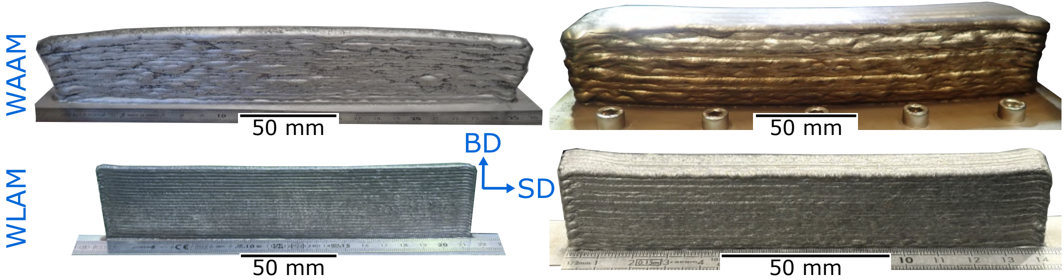

Partial conclusion

- A set of parameters has been identified for single-bead wall manufacturing, taking into account geometrical considerations and maximization of the deposition rate.
- Improper control of the deposition strategy and interlayer cooling times leads to macroscopic deformations in the component.
- The width of the single beads is 3 times larger for WAAM than for WLAM.
- Differences in the shapes of the melt pools → WAAM: predominance of fluid effects.

2. Microstructure and properties

Objective

What are the differences in properties and microstructure between WAAM and WLAM components, and between walls and blocks?

Chemical composition

316L austenitic stainless steel

(wt.%)	Cr	Ni	Mo	Mn	C	N	O	S
Wire	19.20	12.66	2.88	1.78	0.016	0.045	<0.005	0.007
WAAM	18.96	12.50	2.84	1.80	0.014	0.048	0.025	0.007
WLAM	18.40	12.50	2.58	1.35	0.009	0.049	0.12	0.013

Chemical composition (wt.%) (ICP-AES and elementary analysis)

Vaporization of chemical elements during the melting of the wire.
External contaminations during manufacturing.

Inclusions in the manufactured components.
$\Rightarrow$ Importance of the inerting atmosphere.

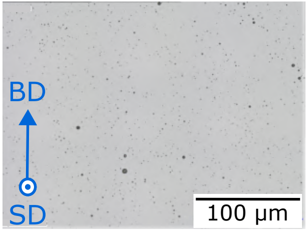

Oxides in the wall (WLAM).

$\Rightarrow$ 3.1. Single-bead walls

3.2. Tiles

Mechanical properties

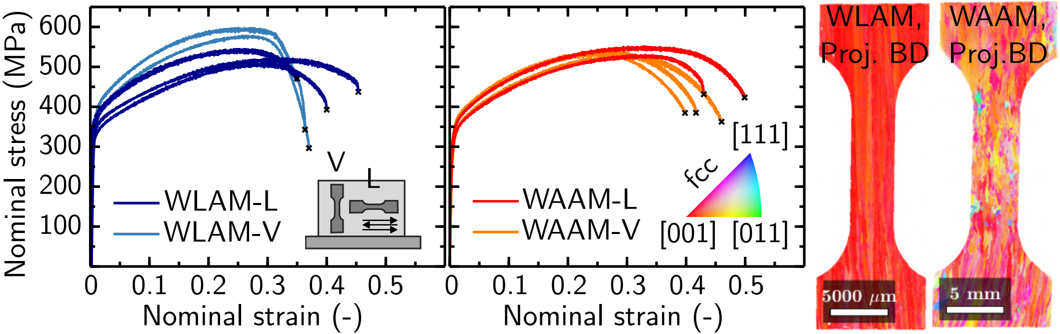

Anisotropy in WLAM; effect of texture and columnar grains.

Requirements for wrought 316L: yield stress: >170 MPa ; tensile strenght: >450 MPa ; ultimate strain: >0.40.

From [ASTM A 473-15].

Microstructure of single-bead walls

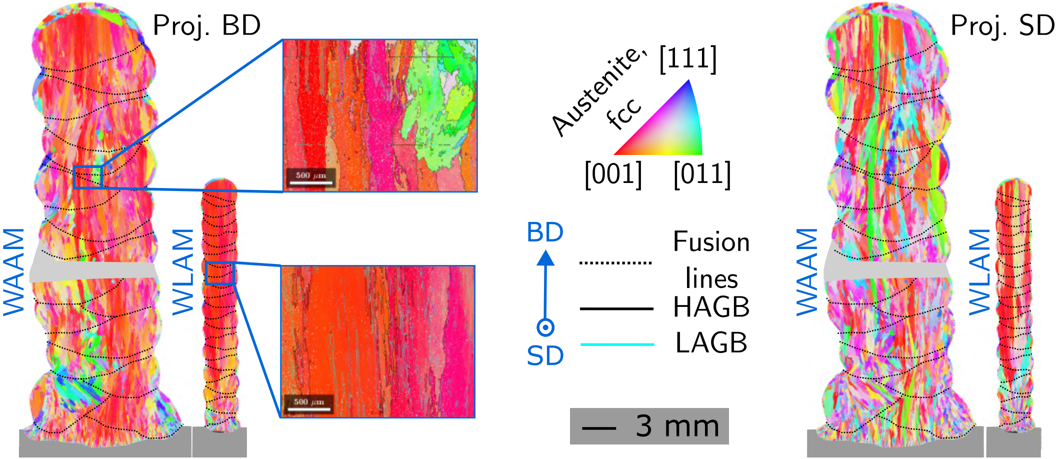

Microstructure of single-bead walls

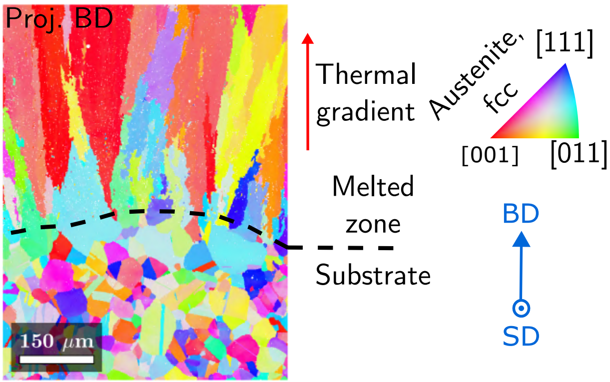

EBSD orientation map of epitaxy in WLAM wall

Thermal gradient:
$10^3 - 10^4$ K/m and $\parallel$ BD.
$\rightarrow$ columnar solidification.

Epitaxy: crystal growth with the orientation of already solidified grains.

Growth competition:
$\langle 001 \rangle_{\parallel}$ thermal gradient
is the preferential orientation for cubic crystals.
$\rightarrow$ Texture

Références : [Mukherjee and DebRoy, 2019a], [Peyre and Charkaluk, 2022]

Solidification structure

Ferrite rate (ferritescope) → WAAM: 8-9%, WLAM: 5-6%

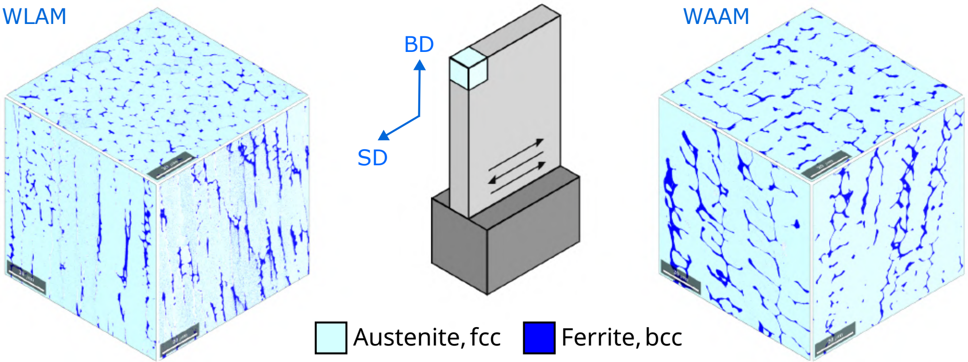

Pseudo-3D EBSD maps of phase composition in single-bead walls

Vermicular ferrite along with the dendritic pattern. → Formed during solidification.

Microstructure - solidification cooling speed relationship

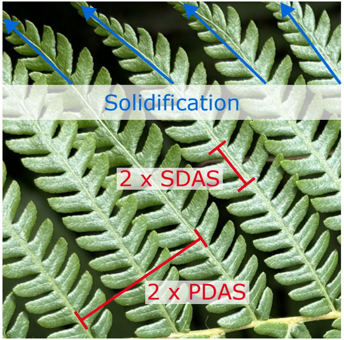

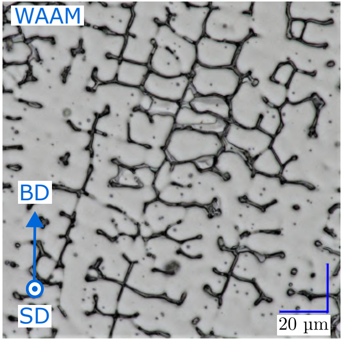

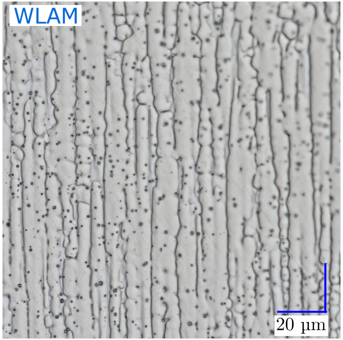

$$\text{PDAS} \sim 80 \times \dot{T}^{-0.33}$$
$$\text{SDAS} \sim 25 \times \dot{T}^{-0.28}$$

From [Katayama and Matsunawa, 1984].

$$\text{WAAM} \rightarrow \dot{T} \sim 100 \text{ K/s}$$
$$\text{WLAM} \rightarrow \dot{T} \sim 1\ 000 \text{ K/s}$$

3.1. Single-bead walls

$\Rightarrow$ 3.2. Tiles

Microstructure of multilayer tiles

Thinner and less elongated grains compared to single-bead walls.

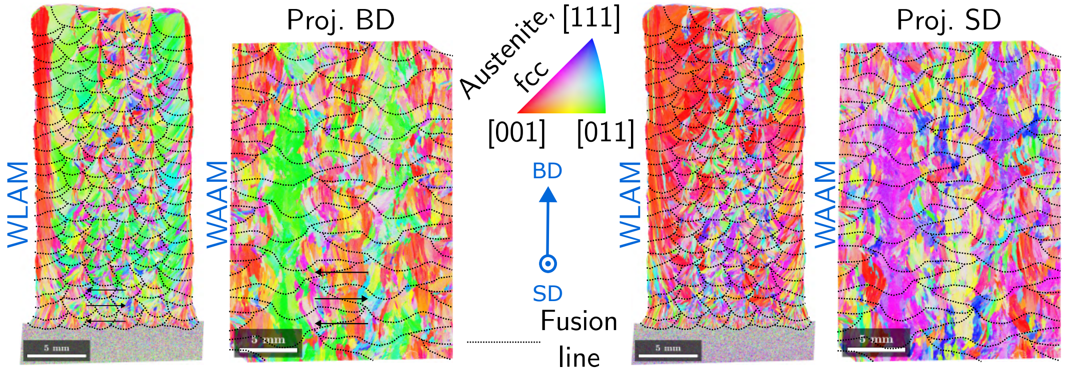

Microstructural variations

Tiles vs single-bead walls: different textures and grains elongation direction.

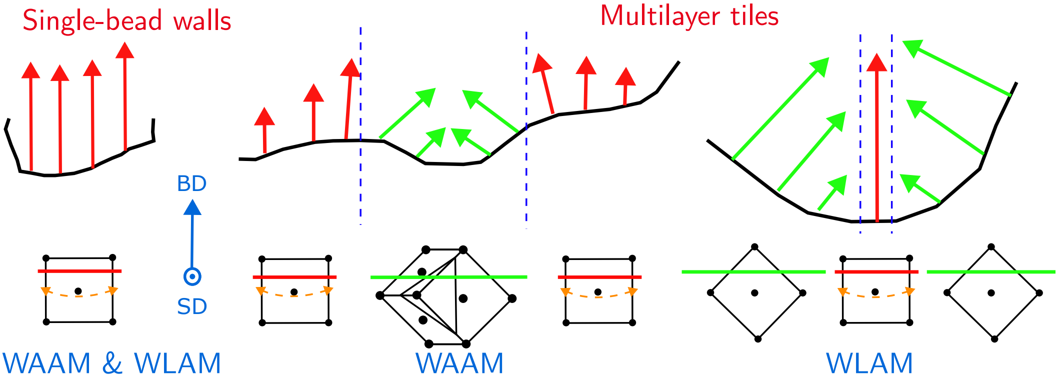

Partial conclusion

Single-bead walls:

- Slight anisotropy of the single-bead walls manufactured by WLAM.
- Tensile properties satisfying the industrial requirements for wrought 316L.
- Elongated and textured grains along $\langle 001 \rangle_{\parallel \text{ BD}}$ $\rightarrow$ thermal gradient direction.
- Cooling rates at solidification $\dot{T}$: WAAM $\rightarrow$ 100 °C/s; WLAM $\rightarrow$ 1000 °C/s.
- The variations between $\dot{T}$ only has a small impact on the mechanical properties.

Multilayer tiles:

- Smaller grains dimension and elongation compared to single-bead walls.
- Two predomining textures: $\langle 001 \rangle_{\parallel \text{ BD}}$ and $\langle 011 \rangle_{\parallel \text{ BD}}$.
- Microstructural variations between tiles manufactured with WLAM and WLAM.
  $\rightarrow$ Differences in the shapes of the melt pools.

4. Finite Element Modeling

Objective

Can a finite element model be developed to simulate both processes?

$\Rightarrow$ 4.1. Implementation of the modeling

4.2. Applications

Implementation of the modeling

Finite element software:

Cast3M

Reproduction of the experimental dimensions.
Clamping of the substrate to the table: springs.
Modeling of the deposition: finite elements addition.

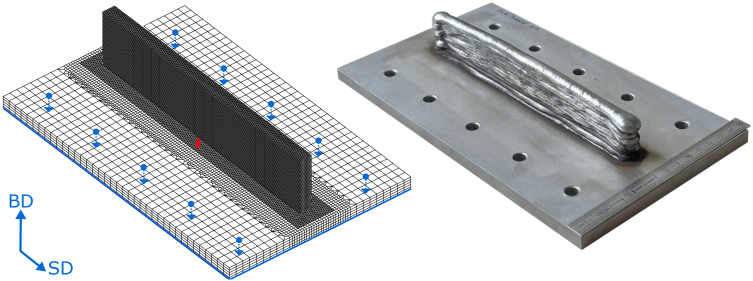

WAAM, comparison of numerical mesh and as-built geometry.

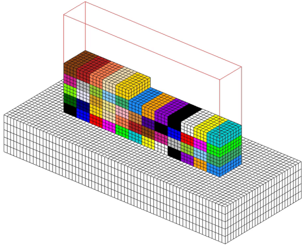

Finite elements addition.

Implementation of the modeling

Parameters for 316L: temperature dependency. From [Depradeux, 2004].
Thermal modeling: conduction, convection, radiation.
Heat source: transverse Gauss volume distribution.
Mechanical modeling: isotropic hardening, no hardening if $T > 1000$ °C.

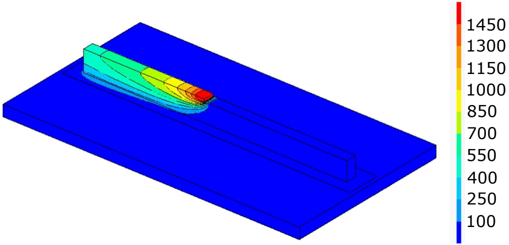

WAAM, temperature (°C)

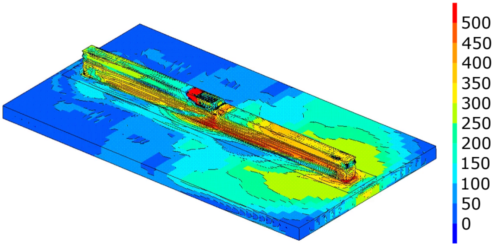

WAAM, von Mises stress (MPa)

Model calibration

Thermocouples-based calibration at 2, 4 and 6 mm from the manufactured walls.

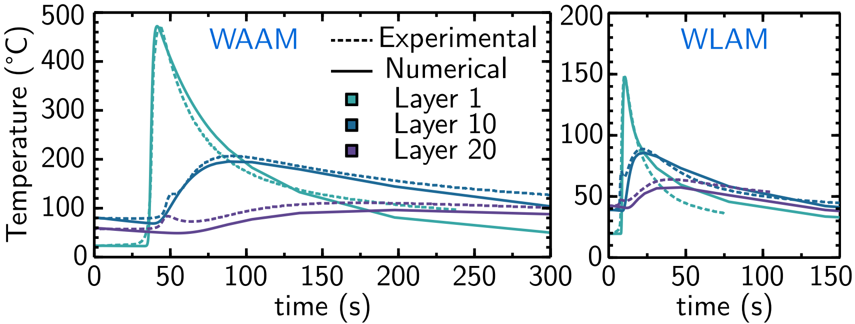

Measured temperature at 4 mm from the walls, 1^{st}, 10^{th} and 20^{th} deposited layers.

Adjusted parameters: convection coefficients, efficiencies of the energy sources, heat sources distribution.

Model calibration

Efficiency coefficients → WAAM: 90%; WLAM: 46%.
Effiency of GTA welding: 77-90%. From [Collings et al., 1979].
Effiency of laser Nd:YAG welding: 38-55%. From [Tadamalle et al., 2014].

Convection coefficient with ambient air: 10 $W.m^{-2}.K^{-1}$.
Heat losses throught the table: 300 $W.m^{-2}.K^{-1}$.

Gauss radius in the manufacturing direction → 0.5 mm.

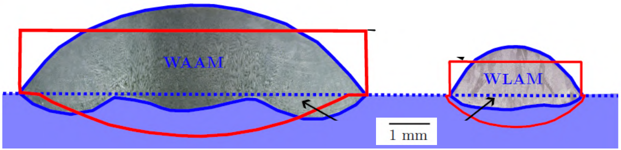

Experimental validation

Accurate reproduction of the temperature field.

→ Allows for qualitative estimation of thermal gradients around the melted zone.

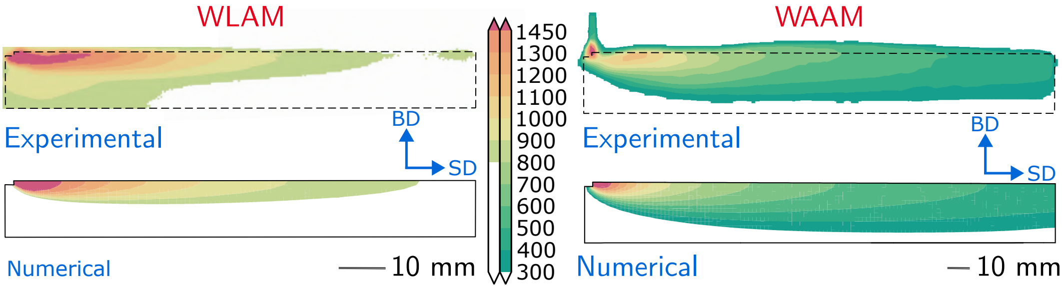

4.1. Implementation of the modeling

⇒ 4.2. Applications

Interlayer cooling time control

Heat accumulation $\longrightarrow$ Geometrical defects.

Excessively long cooling time $\longrightarrow$ Productivity losses.

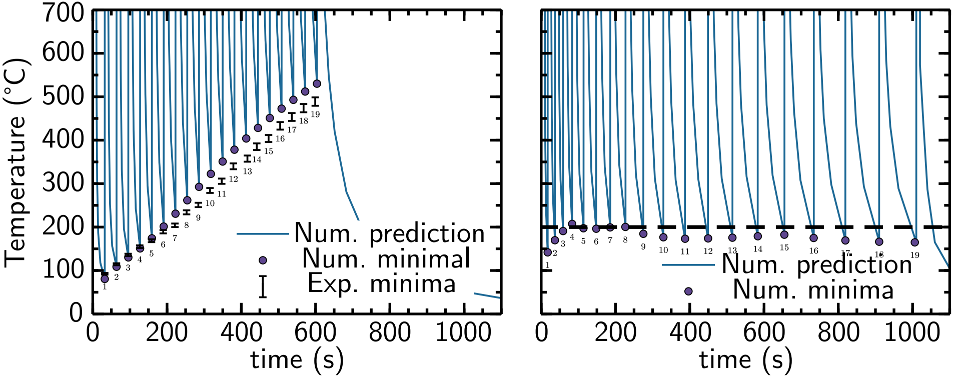

Maximal temperature reached in the wall manufactured by WLAM.

Solidification cooling rate estimation

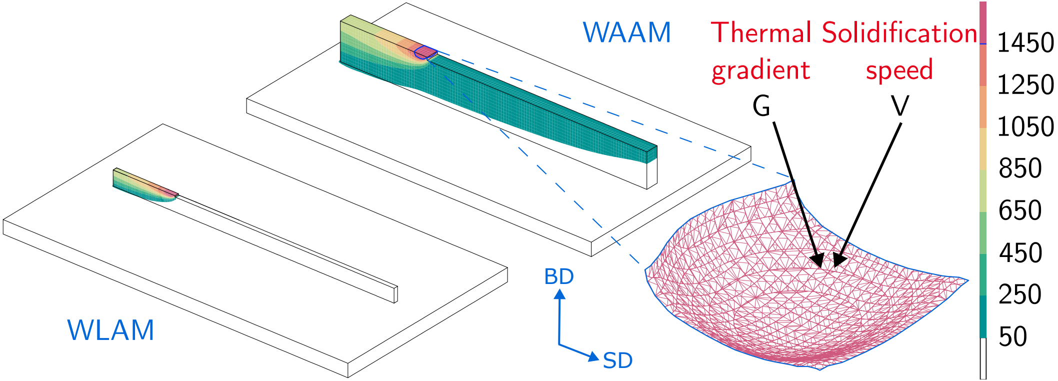

WLAM et WAAM, temperature (°C), mesh of the fusion isotherm.

Solidification cooling rate: $\dot{T} = G \times V$.

Solidification cooling rate control

Couche	WLAM		WAAM	
	Num.	Exp.	Num.	Exp.
1	1800	4000	240	800
10	550	3000	140	120
20	400	1100	110	300

Solidification cooling rates, WAAM et WLAM

Uncontrolled interlayer cooling time

$\rightarrow$ Heat accumulation, variations in $\dot{T}$, variations of the size of dendrites.

Firsts deposited layers

$\rightarrow$ Heat conduction throught the substrate.

Partial conclusion

The developed numerical model allowed for:

- reproducing the thermal and mechanical fields during manufacturing;
- qualitatively estimating the solidification cooling rate evolution;
- determining the interlayer cooling times leading to homogeneous cooling in the successively deposited layers.

A single model developed for two processes with different scales and physics..

5. Conclusion and perspectives

Conclusions

- What are the parameters for manufacturing defect-free components?

  1. WLAM: 3 times thinner deposited layers (3 mm vs 10 mm).
  2. Too small interlayer cooling time $\rightarrow$ macroscopic distortions.

- What are the differences in properties and microstructure between WAAM and WLAM components, and between walls and blocks?

  1. WAAM & WLAM single-bead walls: tensile properties comparable to wrought 316L.
  2. WLAM single-bead wall: slight anisotropy of tensile properties.
  3. WAAM single-bead wall: higher ferrite fraction (8-9% versus 5-6% with WLAM).
  4. 10 times faster solidification cooling rate in the single-bead wall achieved by WLAM.
  5. Influences the dendrite size but not the tensile properties.
  6. Microstructure of thick zones (tiles) different from that of thin sections (walls).

Conclusions

- Can a finite element model be developed to simulate both processes?

1. Satisfactory experimental comparison after thermal calibration.
2. Calibrated parameters: heat losses, distribution and efficiency of the heat source.
3. Selection of the deposition strategy: avoid heat accumulation.
4. Estimation of the minimum interlayer cooling time to ensure homogeneous cooling.
5. Control of the solidification cooling rate.
6. Prevention of microstructural defects: σ-phase formation.

Perspectives

Short term perspectives

1. Determine the tensile properties of tiles.
2. Complete the mechanical characterization of the walls.
3. Characterize the properties of the components after heat treatment.

Long term perspectives

1. Study the manufacturing of more complex geometries: deposition strategies for overlaps, crossings, thickness transitions, etc.
2. Study the implementation of processes for other materials of interest.
3. Adapt the calculation tool to industrial needs: simulation based on manufacturing data and simplification of calculation methods to simulate larger parts.

Thank you for your attention.

Ph.D. student: Damien ARTIÈRES
Supervisors: Sylvain DÉPINOY, Serge PASCAL, Diogo GONÇALVES, Vladimir ESIN

With the contribution of: R. ROBIDET, L. BRIZZI, B.R. ATEBA, L. PEREIRA, H. BADJI, C. METTON, J.-D. BARTOUT, J.-C. TEISSEDRE, L.-T. TRAN HOANG

Thesis conducted at:

1. Paris Saclay University, CEA, Service de Recherche en Matériaux et Procédés Avancés (SRMA)
2. Mines Paris, PSL University, Centre des Matériaux - (CNRS UMR 7633)

References I

Collings, N., Wong, K., and Guile, A. (1979).
Efficiency of tungsten-inert-gas arcs in very-high-speed welding.
Proceedings of the Institution of Electrical Engineers, 126(3):276–280.

Depradeux, L. (2004).
simulation numérique du soudage -acier 316L validation sur cas tests de complexité croissante.
Ph.D. thesis, INSA Lyon.

Frazier, W. E. (2014).
Metal Additive Manufacturing: A Review.
Journal of Materials Engineering and Performance, 23(6):1917–1928.

Katayama, S. and Matsunawa, A. (1984).
Solidification microstructure of laser welded stainless steels.
International Congress on Applications of Lasers & Electro-Optics, 1984(2):60–67.

References II

Levy, G. N., Schindel, R., and Kruth, J. P. (2003).
Rapid manufacturing and rapid tooling with layer manufacturing (LM) technologies, state of the art and future perspective.
CIRP Annals, 52(2):589–609.

Mukherjee, T. and DebRoy, T. (2019a).
A digital twin for rapid qualification of 3D printed metallic components.
Applied Materials Today, 14:59–65.

Mukherjee, T. and DebRoy, T. (2019b).
Printability of 316 stainless steel.
Science and Technology of Welding and Joining, 24(5):412–419.

Peyre, P. and Charkaluk, E. (2022).
La fabrication additive des alliages métalliques 2 – microstructures, post-traitements et propriétés d'usage.
ISTE editions.

References III

Tadamalle, A. P., Reddy, Y. P., Ramjee, E., and Reddy, V. (2014).
Evaluation of Nd: YAG Laser Welding Efficiencies for 304L Stainless Steel.
Procedia Materials Science, 6:1731–1739.